SIMULATION OF THE ROAD-CORRUGATION PHENOMENON

J. G. Riley, Department of Agricultural Engineering, University of Maine at Orono; and
R. B. Furry, Department of Agricultural Engineering, Cornell University

A mathematical model was formulated to simulate the phenomenon of washboarding on unpaved roads. Both the vehicle and the road components were treated as spring-mass-damper assemblies. A digital computer program was written to solve the equations of motion of the system; displacement forcing functions represented irregularities in the path of a moving wheel. The program was executed with varying road and vehicle characteristics, and thus the relations among those primary characteristics and washboard presence and dimensions were established and then verified by physical model tests in the laboratory. In both the simulation and the physical tests, the primary and secondary variables were expressed as dimensionless ratios. Results showed that vehicle weight, tire pressure, and vehicle speed affected primarily the wavelength of the corrugations but that there were maximum or minimum values of those parameters above or below which corrugations would not occur. Results also showed that, for the particular surface materials used, washboarding occurred more readily in a material with a relatively high specific damping capacity and that this property was related to particle shape, effective size, and uniformity coefficient.

•UNPAVED roads subjected to vehicular traffic can, under certain circumstances, suffer from a phenomenon known as washboarding or corrugation, whereby the initially flat road surface becomes deformed into a regular pattern of waves perpendicular to the longitudinal axis of the road. Although the amplitude of the waves is generally only a few inches, the effect on vehicles passing over them is severe, and the usefulness of roads so affected is greatly impaired.

There have been many reports on the occurrence and characteristic forms of washboarding, but there is no one accepted explanation concerning the cause of the problem. Existing theories contain much contradictory information and generally lack solid evidence that would encourage support. It was hypothesized that, if the phenomenon could be simulated mathematically and verified by experimentation, then the mechanism could be explained and the causative factors identified. Thus, a rational basis would be established for work related to practical means of preventing or curing the problem. So that the model developed would be as general as possible, it was decided that the study should attempt to identify all possible pertinent variables and present results in terms of dimensionless groups of those variables

MATHEMATICAL MODELING OF THE ROAD-VEHICLE SYSTEM

The system was treated as a pneumatic-tired wheel running along an initially flat surface layer of granular material on a rigid base. The vehicular component was represented mathematically as a spring-mass-damper system, with a linear spring rate and velocity-dependent damping. Modeling of the loose surface material is a more complex problem because this model must eventually be tied in, from a behavioral aspect, with the vehicle model.

Classical load-sinkage studies for rolling wheels and tracks in soils have always assumed "static" (i.e., slow) loading conditions (2, 4). Physical observations of washboarding, however, showed that it is a phenomenon involving impact loading and that velocity is indeed critical. If rate of loading is to be considered, then, according to

Bekker (1), the soil forces produced by an impact may be thought of as the sum of the static force and additional forces resulting from viscocity and acceleration of the soil mass. For a plate-sinkage test, as a first approximation,

$$F_s = f_1(Z) + f_2(Z, \dot{Z}) + F_3(Z, \ddot{Z}) \tag{1}$$

where

F_s = soil force acting on the plate,
Z = penetration of the plate,
$\dot{Z}$ = velocity of the plate, and
$\ddot{Z}$ = acceleration of the plate.

It is obvious from this equation that the soil mass is, in the broadest sense, being treated as a spring-mass system with damping. Such a representation of soil has been used in the study of earthquakes and wave propagation for many years, generally because of the difficulty of describing dynamic behavior satisfactorily by any other method.

Rickman (10) outlines techniques for describing materials by means of a spring and dashpot, representing respectively the elastic and viscous components. To accurately describe the behavior of nonhomogeneous soils requires the incorporation of large numbers of spring and dashpot pairs (6, 7, 14); but for a single homogeneous layer of granular material resting on a rigid base, it is reasonable to use a single spring-dashpot pair. The nonlinearity of static load-deflection curves for any granular material, however homogeneous it may be, necessitates the use of empirical load-deflection data to represent the nonlinear spring; that precludes any possibility of an explicit analytical solution to the problem but makes for a much simpler model.

If the mass of soil accelerated is to be considered as a contributing factor to total soil reaction force, then some means of representing that soil mass must be established. Because the soil under the wheel is being treated as a spring-dashpot pair, then the effective mass of that soil will be calculated in the same way that the effective mass of a spring is computed. If the analysis described by Phelan (9) is followed, the accelerated mass of soil will be represented in the model by one-third of the mass under the contact patch of the tire, as determined by the area of this contact patch, the depth of material, and the material's mass density.

The models for the vehicle and road surface are combined in the composite model that is represented as a 2-deg-of-freedom system and shown in Figure 1.

Although the wheel is in contact with the road, the system is governed by the following equations:

$$m_1\ddot{x}_1 = k_1(x_2 - x_1) + c_1(\dot{x}_2 - \dot{x}_1) \tag{2}$$

$$m_2\ddot{x}_2 = k_1(x_1 - x_2) + c_1(\dot{x}_1 - \dot{x}_2) + k_2(y - x_2) + c_2(\dot{y} - \dot{x}_2) \tag{3}$$

for $(x_1 - x_2) \leq \delta_{st}$, where δ_{st} is static tire deflection.

When the wheel leaves the surface, it moves in a trajectory whose path, neglecting air resistance, is governed by

$$\dot{x}_1 = \dot{x}_{1p} - gt \tag{4}$$

for $(x_1 - x_2) > \delta_{st}$, and where

$\dot{x}_{1p}$ = vertical velocity of projection,
g = acceleration due to gravity, and
t = time measured from the instant of projection.

In the horizontal plane, as the vertical reaction force on the tire changes, so will the effective rolling radius. For a towed wheel tending to rotate at constant angular velocity, this results in slippage i defined by

$$i = 1 - \frac{R}{R_{st}} \tag{5}$$

where

R = effective rolling radius, and
R_{st} = static rolling radius.

If the tire contact patch length is L and if the tire perimeter rolls out a distance L, then the axle of the wheel moves a distance L(1 - i), and the tire contact patch moves relative to the ground a distance -iL, where motion is forward, i.e., skid. Motion of the contact patch on the ground results in horizontal shear of the soil, which in turn results in vertical sinkage. Bekker showed that the relation between horizontal and vertical loads and the corresponding deformations could be expressed by

$$\frac{\tau_{max}}{p - p_{cr}} = \frac{J}{Z_J} \tag{6}$$

where τ_{max}, the maximum shear stress, is given by

$$\tau_{max} = c + p \tan \phi \tag{7}$$

and

p = vertical load per unit area,
c = cohesion of the soil,
ϕ = angle of internal shearing resistance,
J = horizontal deformation, and
Z_J = vertical deformation due to horizontal deformation only.

p_{cr} is Terzaghi's (12) bearing-capacity value defined semi-empirically as

$$p_{cr} = cN_c + \gamma[N_q (Z_s + Z_J) + \tfrac{1}{2} b N_\gamma] \tag{8}$$

where N_c, N_q, and N_γ are dimensionless ratios depending only on ϕ, and where

γ = specific weight of the material,
b = width of the contact patch, and
Z_s = sinkage due to vertical load only.

Combining Eqs. 6, 7, and 8 yields

$$Z_J = \frac{J[p - cN_c - \gamma (N_q Z_s + \tfrac{1}{2} b N_\gamma)]}{c + p \tan \phi + \gamma N_q J} \tag{9}$$

Thus, total vertical deformation Z_o is defined by

$$Z_o = Z_s + Z_J \tag{10}$$

APPLICATION OF DIMENSIONAL ANALYSIS

Concurrent with the mathematical modeling of the phenomenon, all possible relevant vehicle and surface material parameters were identified and arranged in dimensionless groups, according to the laws of dimensional analysis, in order to facilitate an understanding of the specific effects of a particular variable, both in the mathematical solution and in tests on the physical model.

Vehicle characteristics are fairly easily identified, consisting of the mass of the wheel, the tire spring rate and damping coefficient, tire width and geometry, and vehicle speed. Identification of pertinent surface material characteristics is more difficult because, in general, dynamic soil properties have not been successfully defined. The most complete listing of basic properties is given by Hansen (5). The discarding of variables not applicable to this situation results in the list given in Table 1.

The secondary variables, wavelength and amplitude of the washboarding, may be expressed as some unknown function of the primary variables.

$$L = f_1 (W, k_1, \zeta_t, b, d, v, g, n, t, \gamma, c, \phi, s, C_u, \zeta_s, \sigma, \lambda, h) \quad (11)$$

$$A = f_2 (W, k_1, \zeta_t, b, d, v, g, n, t, \gamma, c, \phi, s, C_u, \zeta_s, \sigma, \lambda, h) \quad (12)$$

A dimensional analysis then yields the following results:

$$\frac{L}{s} = F_1 \left(\frac{W}{cs^2}, \frac{k_1}{cs}, \zeta_t, \frac{b}{s}, \frac{d}{s}, \frac{v}{g^{1/2} s^{1/2}}, n, \frac{t}{s}, \frac{\gamma s}{c}, \phi, C_u, \zeta_s, \sigma, \frac{\lambda}{s}, \frac{h}{s} \right) \quad (13)$$

$$\frac{A}{s} = F_2 \left(\frac{W}{cs^2}, \frac{k_1}{cs}, \zeta_t, \frac{b}{s}, \frac{d}{s}, \frac{v}{g^{1/2} s^{1/2}}, n, \frac{t}{s}, \frac{\gamma s}{c}, \phi, C_u, \zeta_s, \sigma, \frac{\lambda}{s}, \frac{h}{s} \right) \quad (14)$$

These dimensionless groups were used to guide the physical test procedure in the evaluation of the mathematical model and in the investigation of the relative contribution of certain variables to the occurrence of form of washboarding. A listing of these groups or pi terms is given below:

$$\pi_{1a} = L/s \qquad \pi_4 = \zeta_t \qquad \pi_8 = n \qquad \pi_{12} = C_u$$
$$\pi_{1b} = A/s \qquad \pi_5 = b/s \qquad \pi_9 = t/s \qquad \pi_{13} = \zeta_s$$
$$\pi_2 = W/cs^2 \qquad \pi_6 = d/s \qquad \pi_{10} = \gamma s/c \qquad \pi_{14} = \sigma$$
$$\pi_3 = k_1/cs \qquad \pi_7 = v/(g^{1/2} s^{1/2}) \qquad \pi_{11} = \phi \qquad \pi_{15} = \lambda/s$$
$$\pi_{16} = h/s$$

A substantial number of parameters required definition, and that was accomplished by separate testing procedures described in detail by Riley (11). Table 2 gives measured properties of the 3 sands used in the tests. Cohesion and angle of shear were measured with a torsional shear device; effective size and coefficient of uniformity were found by performing a mechanical analysis for each sand; and dumping capacity was measured from the decay of free vibrations for the sand contained in a rubber membrane and subjected to an instantaneous loading condition.

COMPUTER SIMULATION AND PHYSICAL TEST PROGRAM

The mathematical model of the phenomenon allows for prediction of road profile changes as a function of a large number of variables, the values for some of which must be introduced as empirical data. The process of washboarding is a multipass phenomenon; therefore, for prediction of the road profile after a number of passes, the profile resulting from one pass of the wheel becomes the input profile for the next pass and so on. Because of the nonlinearities and the semi-empirical nature of the model, an analytical solution is impossible, and a digital computer solution using numerical methods must be employed.

The physical model constructed in the laboratory consisted of a 6-ft diameter circular track around which a small pneumatic-tired wheel was propelled by a rotating arm driven from the center of the track by an electric motor and reduction gearbox. A schematic diagram of the apparatus is shown in Figure 2. Tests were made on this model with the same values for the variables as those used for computer input. Washboard amplitude and wavelength from peak to peak were measured. Experimental data from these physical tests were then plotted on the graphs obtained from the computer simulation for comparison of actual and predicted results. The flow chart for the simulation, along with a FORTRAN IV program listing and typical prediction model output, is given by Riley (11).

RESULTS AND DISCUSSION

Figure 3 shows the computer prediction of the surface profile after the third, sixth, ninth, and twelfth passes of the wheel. Values for the system variables for this test

Figure 1. Schematic diagram of road-vehicle system.

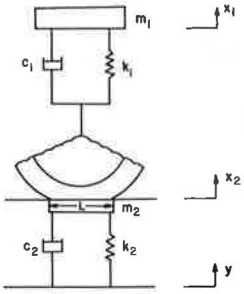

L = length of contact patch.
m_1 = mass of wheel and added weights.
m_2 = effective mass of surface material.
k_1 = spring rate of tire.
k_2 = effective spring rate of surface material.
c_1 = tire damping coefficient.
c_2 = surface material damping coefficient.
x_1 = axle displacement.
x_2 = surface displacement.
y = displacement forcing function (pre-existing profile.)

Table 1. Pertinent quantities for road and vehicle.

Variable	Symbol	Units	Dimensions[a]
Secondary			
Wavelength of washboarding	L	Ft	L
Amplitude of washboarding	A	Ft	L
Primary			
Total static weight on wheel[b]	W	Lb	F
Tire spring rate	k_1	Lb/ft	FL^{-1}
Tire damping capacity	ζ_1	—	—
Tire width	b	Ft	L
Tire diameter	d	Ft	L
Vehicle velocity	v	Ft/sec	LT^{-1}
Acceleration due to gravity	g	Ft/sec^2	LT^{-2}
Number of passes	n	—	—
Surface material layer thickness	t	Ft	L
Specific weight	γ	Lb/ft^3	FL^{-3}
Apparent cohesion	c	Lb/ft^2	FL^{-2}
Angle of shearing resistance	ϕ	—	—
Effective size	s	Ft	L
Coefficient of uniformity	C_u	—	—
Material damping capacity	ζ_s	—	—
Particle shape	σ	—	—
Length of initial irregularity	λ	Ft	L
Height of initial irregularity	h	Ft	L

[a]Basic dimensions used in this study are F, force; L, length; and T, time.
[b]Including weight of tire, rim, and suspension components.

Table 2. Measured properties of test sands.

Sand	σ	s (mm)	C_u	ζ_s	c ($lb/in.^2$)	ϕ (deg)	γ (lb/ft^3)	N_c	N_q	N_γ
A	Angular	0.045	2.2	0.8	0.1	31	82.2	40	24	23
B	Spherical	0.310	1.4	0.2	0.1	26	93.0	27	15	13
C	Angular	0.080	1.7	0.3	0.1	28	78.9	33	18	19

Figure 2. Schematic diagram of test facility.

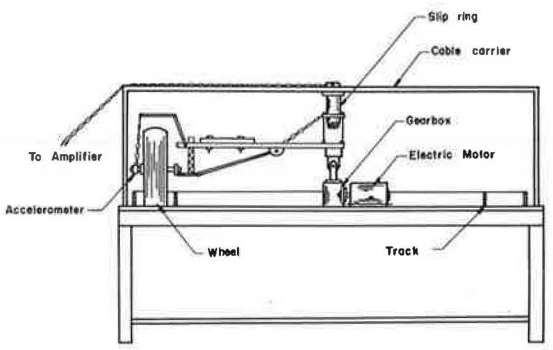

Figure 3. Computer prediction of developing profile.

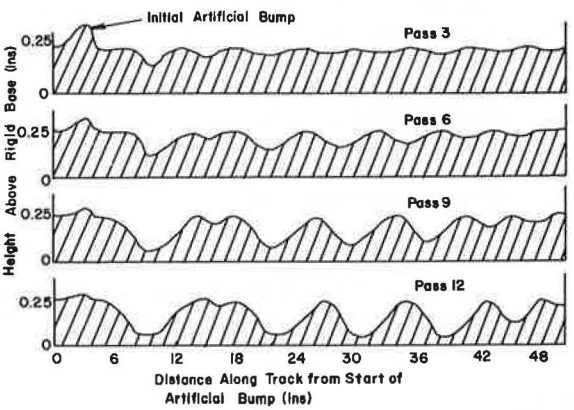

are listed below:

$W = 10.25$ lb	$d = 0.83$ ft	$\gamma = 82.2$ lb/ft^3	$C_u = 2.2$
$k_1 = 2{,}736$ lb/ft	$v = 5$ ft/sec	$c = 14.4$ lb/ft^2	$\zeta_s = 0.8$
$\zeta_t = 0.17$	$g = 32.2$ ft/sec^2	$\phi = 31$ deg	σ = angular
$b = 0.25$ ft	$t = 0.0208$ ft	$s = 0.00015$ ft	$\lambda = 0.33$ ft
			$h = 0.0208$ ft

After only 3 wheel passes, washboarding is present for a considerable distance beyond the initial irregularity; further passes amplify the corrugations while simultaneously shifting the whole pattern in the direction of the wheel's travel. By about the ninth pass, a steady-state amplitude and wavelength condition is reached, after which further passes merely cause a continued forward migration of the developed pattern.

Figure 4 shows a comparison of the predicted and measured profiles for the third and ninth passes of this first test; the values for the various parameters are the same as those given above. There is close agreement between predicted and experimental results, even to the duplication of the first deep depression, the second small one, and the flattening out of the initial irregularity.

Initial qualitative tests on the physical model led to the identification of certain vehicle parameters as having marked effects on the nature of the corrugations, and the second part of the computer simulation involved the study of some of those effects. The particular parameters chosen were tire pressure, weight on the wheel, and vehicle speed. Values for those were varied independently and read into the computer; sufficient wheel passes were made so that the steady-state condition was reached; and the resulting output profile was then interpreted simply as 2 numerical values representing amplitude and wavelength. For a particular tire inflation pressure, i.e., with π_3 constant, the wavelength of the corrugations decreases linearly with increasing weight on the wheel up to a certain weight, after which the decrease becomes essentially exponential. Similarly, under the conditions of testing, for tire inflation pressures between 10 and 30 lb/in.^{2}, washboard wavelength decreases linearly with increasing tire spring rate for constant weight on the wheel. The 3-dimensional representation shown in Figure 5 gives a qualitative description of the relations between those particular pi terms within the given limits. As a generalization, one can say, with all other factors constant and within the range of testing, that high tire pressure and heavy weight on the wheel produce washboarding with a short wavelength and that low pressure and light weight yield a longer wavelength.

Figure 6 shows that, all other parameters being constant, wavelength increases essentially linearly with vehicle velocity within the range of testing, a predictable result and one that agrees completely with the work of other investigators (3, 8).

For given surface material characteristics, if washboarding occurred at all, it did so through wide variation of tire pressure, weight on the wheel, and wheel speed; and its wavelength was directly related to values of those parameters. However, there were certain limiting values for them below or above which washboarding did not occur.

If washboard amplitude, expressed as the pi term A/s, is plotted against the vehicle pi terms, then it is reasonable to select a value for A/s above which washboarding is considered to be present. The value chosen in these tests was A/s = 100, a figure that represented the approximate point where washboarding became readily visible to the naked eye. The independent pi terms are then plotted against one another to show the cutoff points and, thus, define an area within which any combination of the 2 plotted dimensionless variables will result in washboarding. If this is done with 3 independent pi terms, the result is a solid defined region within which washboarding will occur for the given tire, surface, and test conditions.

Results of that procedure are shown in Figure 7. Translated into practical terms, they show, for example, that for this physical system, with all other parameters constant, washboarding will not occur below a vehicle speed of 3.2 ft/sec ($\pi_7 = 46.41$), above a wheel weight of 30 lb ($\pi_2 = 95.59 \times 10^6$), or below a tire spring rate of 100 lb/in. ($\pi_3 = 56.45 \times 10^4$). The lower limit of wheel weight and the upper limit of tire pressure, both expressed as pi terms, are not in fact cutoff points but merely the limiting values

Figure 4. Comparison of measured and predicted profiles.

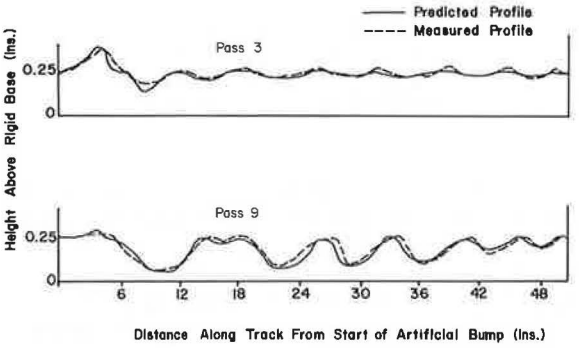

Figure 5. Wavelength as a function of wheel weight and tire inflation pressure, expressed as dimensionless ratios.

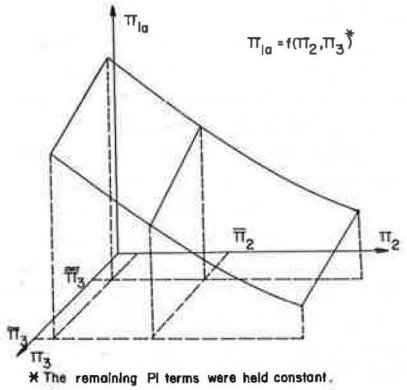

Figure 6. Wavelength as a function of wheel weight and vehicle speed, expressed as dimensionless ratios.

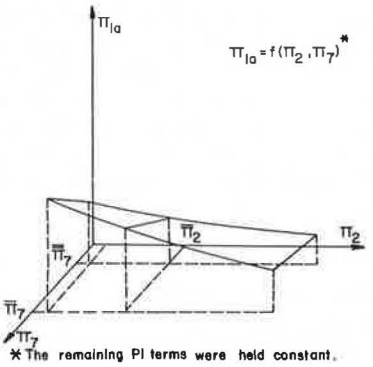

Figure 7. Washboard occurrence as a function of wheel weight, vehicle speed, and tire inflation pressure, expressed as dimensionless ratios.

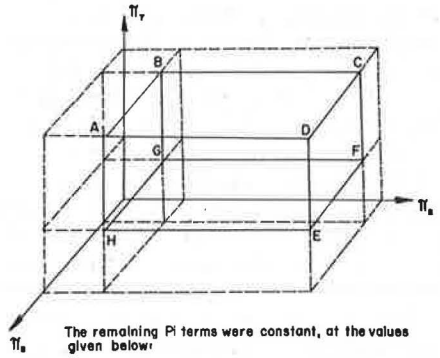

The remaining PI terms were constant, at the values given below:

$\bar{\pi}_4 = 0.17$	$\bar{\pi}_9 = 140.89$	$\bar{\pi}_{13} = 0.8$
$\bar{\pi}_5 = 1693$	$\bar{\pi}_{10} = 0.0008427$	$\bar{\pi}_{14}$ = Angular
$\bar{\pi}_6 = 5622.16$	$\bar{\pi}_{11} = 31$	$\bar{\pi}_{15} = 1693$
$\bar{\pi}_8 = 50$	$\bar{\pi}_{12} = 2.2$	$\bar{\pi}_{16} = 140.89$

for which experimental data were taken (i.e., beyond the resultant pi term values, washboarding certainly might occur; but since tests were not run for verification, that fact cannot be stated categorically).

These results indicated that the proposed mathematical model provides a good representation of the phenomenon and leads to an understanding of the effects of the vehicle characteristics on the form of the washboarding. It is now appropriate to consider how surface material characteristics influence the phenomenon, especially the reason for causing the occurrence of washboarding in one material but not in another.

Two of the test sands, A and B, showed completely different behavior in that with all other parameters constant one washboarded markedly and the other did not do so at all. Both sands had approximately the same angle of internal shearing resistance ϕ and cohesion c and, therefore, about the same resistance to horizontal shear but widely differing vertical load-deformation curves and damping capacities. When the wheel lands after a bump, however small, there is a slip-sinkage effect. Both sands deform to the same extent because of this; but then, as the wheel rides up the bump resulting from this sinkage, different behavior results. Sand B, with a low damping capacity ($\zeta_s = 0.2$), is deformed by the vertical tire forces so that the wheel is not reprojected into the air but merely continues on the level, forming a flat rut. Sand A, however, with a high damping capacity ($\zeta_s = 0.8$), offers higher resistance to the dynamic vertical forces so that the bump is not totally flattened and the tire is projected into the air to continue the propagation process.

If the measured properties of the sands given in Table 2 are considered, it is seen that, proceeding from sand A through C to B (i.e., yielding washboarding, slight washboarding, and no washboarding respectively), the decrease in damping capacity is accompanied by a decrease in uniformity coefficient and an increase in effective size. That is in agreement with the work of Tschebotarioff and McAlpin (13), who found that low damping capacity was associated with poor gradation for certain sands. It would appear then that materials with a low modulus of sinkage and low damping capacity are incapable of supporting vehicle-induced corrugation and that those characteristics are related to gradation.

However, the susceptibility of some uniform materials to washboarding indicates that gradation alone is not the deciding factor but that some other geometric property is important. For these tests, the geometry of each sand was summarized by σ, s, and C_u. Although this would seem to be an intuitively reasonable method, for a full understanding of the reason for different materials having different damping capacities and, thus, different washboard supporting capabilities, further study is required to identify relevant basic soil properties that would more accurately describe the material.

SUMMARY AND CONCLUSIONS

A mathematical model was constructed to simulate the phenomenon of washboarding on unpaved roads. The road-vehicle system was modeled as a 2-deg-of-freedom mass-spring-damper system, the vertical vibrations of which were described by 2 second-order differential equations. Horizontal displacements were calculated from the change in tire rolling radius and soil mechanics slip-sinkage theory. A digital computer program was written to solve those equations and thus predict the changes in road profile as the wheel rolls along the road.

Varying road and vehicle characteristics were used as input to the program, and the relations between primary vehicle characteristics and washboard presence and dimensions were calculated and verified by physical model tests in the laboratory. For a particular wheel, the vehicle weight, tire inflation pressure, and speed affect primarily the wavelength of the washboard, and amplitude is a function mainly of the loose layer thickness. There were, however, maximum or minimum values of the vehicle parameters above or below which corrugations would not occur. As far as the characteristics of the loose surface layer are concerned, it was shown that for the 3 sands tested washboarding occurred more readily in the well-graded sand, which had a higher damping capacity and greater resistance to dynamic vertical deformation than the less well-graded sands, even though the soil strength parameters of cohesion and angle of internal shearing resistance were approximately the same.

Even though that was a theoretical analysis, it indicates conditions that would not be favorable to washboard formation in the real world. Concerning the vehicle, all that can be recommended practically is that vehicle speeds be kept low on roads proven to be susceptible to corrugation; high wheel weight aids prevention, but that would not seem to be a feasible method in practice. Concerning road materials, if it were possible to increase shear strength to prevent or reduce horizontal shear, or decrease damping capacity so that the bumps would not withstand dynamic wheel forces, then washboarding would not form.

Shear strength can be increased sufficiently to prevent washboarding by paving or asphalting the road for an adequate depth or more practically by increasing cohesion either by application of a binder or by use of a well-graded material with a reasonable proportion of clay. Low specific damping capacity can be most easily achieved, at least in sand, by using a material with little gradation, i.e., having a uniform particle size; however, such a material, although not sustaining washboarding, will allow high wheel sinkage and cause high rolling resistance. It is, therefore, a cure of questionable value. Scraping down and flattening existing washboarding is at best a temporary measure only and at worst an exercise in futility; for, if the road surface material is conducive to the formation of corrugations, then under wheeled traffic the flat surface represents an unstable condition. If the corrugations are merely scraped flat, the road will simply begin to washboard again until the stable corrugated form is reached once more.

Considering the millions of miles of unpaved roads that are susceptible to washboarding, any selection of special road surface material or treatment of existing material must be considered from an economic viewpoint; there is certainly no simple, cheap, and effective means of controlling the problem.

REFERENCES

1. Bekker, M. G. Off the Road Locomotion. Univ. of Michigan Press, Ann Arbor, 1960.
2. Bernstein, R. Probleme zur experimentallen Motorpflugmechanik. Vol. 16, Munich, 1913.
3. Dana, H. J. Formation of Washboards in Gravel Highways. HRB Proc., Vol. 9, 1929, pp. 186-208.
4. Gill, W. R., and Vanden Berg, G. E. Soil Dynamics in Tillage and Traction. U.S. Department of Agriculture, Agricultural Handbook 316, 1967.
5. Hansen, R. The Potential for Similitude and Dimensional Analysis in the Design of Flexible Pavements. Cornell Univ., MS thesis, 1966.
6. Kondner, R. L., and Ho, M. M. K. Complex Modulus of a Cohesive Soil From Stress Relaxation Response Using the 1-Sided Fourier Transform. Jour. Applied Physics, Vol. 36, 1965.
7. Krizek, R. J. Phenomenological Soil-Polymer Parallels. Am. Sci., Vol. 56, 1968.
8. Mather, K. B. The Cause of Road Corrugations and the Instability of Surfaces Under Wheel Action. Civil Engineering and Public Works Review, London, Vol. 57, No. 670, 1962.
9. Phelan, R. M. Dynamics of Machinery. McGraw-Hill, New York, 1967.
10. Rickman, R. W. Sonic Radiation for Soil Mechanical Property Measurement. ASAE, Minneapolis, Paper 70-344, 1970.
11. Riley, J. G. The Road Corrugation Phenomenon: A Simulation and Experimental Evaluation. Cornell Univ., PhD thesis, 1971.
12. Terzaghi, K., and Peck, R. B. Soil Mechanics in Engineering Practice. John Wiley and Sons, New York, 1948.
13. Tschebotarioff, G. P., and McAlpin, G. W. Vibratory and Slow Repetitional Loading of Soils. HRB Proc., Vol. 26, 1946, pp. 551-562.
14. Waldron, L. J. Soil Viscoelasticity: Superposition Tests. Proc., Soil Sci. Soc. of Am., 1964.